Electrochemical investigation of the energetics of irradiated FeS2 (pyrite) particles

Guancheng Chen, Jyh Myng Zen, Fu Ren F. Fan, and Allen J. Bard

J. Phys. Chem., **1991**, 95 (9), 3682-3687 • DOI: 10.1021/j100162a045

Electrochemical Investigation of the Energetics of Irradiated FeS_2 (Pyrite) Particles

Guancheng Chen,† Jyh-Myng Zen,‡ Fu-Ren F. Fan, and Allen J. Bard*

Department of Chemistry, The University of Texas at Austin, Austin, Texas 78712
(Received: December 19, 1989; In Final Form: December 3, 1990)

The band energies of FeS_2 particles (~10 μm) were estimated by collection of electrons generated by irradiation of the particles in the presence of a hole acceptor (e.g., tartrate ion) at an inert collector electrode. Electrons were collected directly from the particles or by the mediator $Ru(NH_3)_6^{3+}$, where the resulting +2 state is oxidized at the electrode. The variation of the steady-state photocurrent in the presence of mediator as a function of pH allowed estimation of the quasi-Fermi level for electrons and located the conduction and valence band edges at −0.1 and +0.9 V vs SCE, respectively, at pH 0, and −0.9 and +0.1 V vs SCE, respectively, at pH 14. Modification of the FeS_2 surface with Pt produced a small (ca. 0.1 V) negative shift in the potential for photocurrent onset.

Introduction

We report here electrochemical studies of irradiated suspensions of FeS_2 particles that yield estimates of their band energetics and relative efficiencies of photoreactions. Transition-metal chalcogenides have been shown to be promising semiconductor electrodes in photoelectrochemical (PEC) cells.[1,2] FeS_2 (pyrite) was introduced by Tributsch and co-workers[1,3,4] as an electrode in PEC cells, and it has also been proposed as an anode depolarizer for H_2 production[5] and as a cathode in high-energy-density batteries.[6] The reported value for the band gap of bulk FeS_2 is about 1 ± 0.2 eV.[3,7-15] Thus, FeS_2 absorbs light in the whole visible region, which makes it attractive for solar energy applications. Moreover, this semiconductor material is composed of cheap, abundant, nontoxic elements. There have been a number of studies of the semiconducting and electrochemical properties of FeS_2. Many of these deal with the electrochemical behavior of natural pyrite crystals in the dark.[16-20] Several groups have studied solid-state properties of pyrite, using both natural and synthetic samples.[7,9,15,21-23] While PEC studies of synthetic photoactive FeS_2 single-crystal electrodes have been carried out, there have been few studies of the photoelectrochemical behavior of FeS_2 particles.[24] Differences between a semiconductor electrode and semiconductor particles have been discussed.[25-30] The photocatalytic action of illuminated semiconductor particles immersed in an electrolyte solution can be understood in terms of photoinduced electron/hole (e^-/h^+) pair separation, followed by reduction and oxidation (charge-transfer) reactions with components on the particle surface or in the solution.[25,26] Previous reports from our group discussed the use of electrochemical measurements in which photogenerated charge at semiconductor particles was collected at an inert metal electrode immersed in irradiated suspensions, e.g., those of TiO_2, CdS, WO_3, and Fe_2O_3.[31-34] For example, irradiation of a semiconductor particle in the presence of a species that is irreversibly oxidized by photogenerated holes in the particle (i.e., a sacrificial electron donor) produces a particle with excess electrons. When the particle touches an inert electrode held at the appropriate potential, these electrons are transferred to the electrode to produce an anodic current (Scheme IA). Enhanced photocurrents are observed in the presence of small quantities of an electron acceptor, such as the methyl viologen dication (MV^{2+}). Here electrons are transferred from the particle to MV^{2+} to produce $MV^{+\bullet}$, which is, in turn, oxidized at the collector electrode (Scheme IB). Previous studies of semiconductor particles by this electrochemical method were carried out on materials with rather large band gaps. We thought it of interest to extend this experimental approach to a small-band-gap material, FeS_2. We describe the use of several hole acceptors (sacrificial donors), e.g., tartrate and sulfide, and electrochemical measurements of FeS_2 suspensions with and without MV^{2+} or $Ru(NH_3)_6^{3+}$ as an electron acceptor and discuss the effect of light intensity and pH on the

SCHEME I

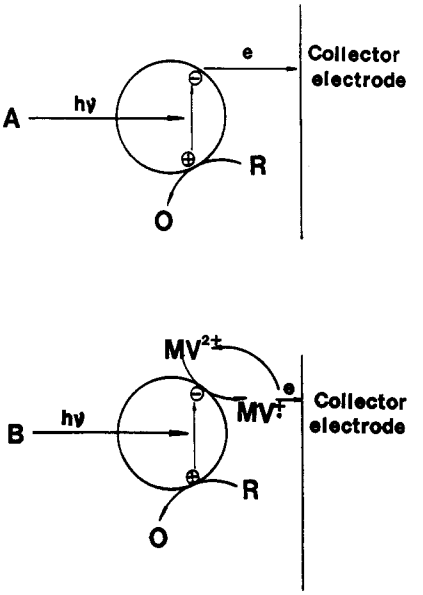

†Current address: Qinghai Institute of Salt Lakes, Xining, Qinghai, People's Republic of China.

‡Current address: Department of Chemical Engineering, The University of Texas at Austin, Austin, TX 78712.

(1) Tributsch, H. *Struct. Bonding (Berlin)* **1982**, *49*, 127.
(2) Schneemeyer, L. F.; Wrighton, M. S. *J. Am. Chem. Soc.* **1979**, *101*, 6496.
(3) Ennaoui, A.; Fiechter, S.; Jaegerman, W.; Tributsch, H. *J. Electrochem. Soc.* **1986**, *133*, 97.
(4) Jaegermann, W.; Tributsch, H. *J. Appl. Electrochem.* **1983**, *13*, 743.
(5) Lawani, S. B.; Shami, M. *J. Electrochem. Soc.* **1986**, *133*, 1364.
(6) Vincent, C. A. *Modern Batteries*; Edward Arnold Ltd.: London, 1984; p 182.
(7) Bither, T. A.; Bouchard, R. J.; Cloud, W. H.; Donohue, P. C.; Siemons, W. *Inorg. Chem.* **1968**, *7*, 2208.
(8) Liu, C.-Y.; Pettenkofer, C.; Tributsch, H. *Surf. Sci.* **1988**, *204*, 537.
(9) Marinace, J. C. *Phys. Rev.* **1954**, *96*, 593.
(10) Sasaki, A. *J. Mineral. Soc. Jpn.* **1955**, *1*, 290.
(11) Otsuka, R. Synopsis, Graduate School of Science and Engineering, Waseda University, Waseda, Japan, 1957; pp 6, 57.
(12) Fukui, J. *J. Phys. Soc. Jpn.* **1970**, *31*, 1277.
(13) Gupta, V. P.; Ravindra, N. M.; Srirastava, V. K. *J. Phys. Chem. Solids* **1980**, *41*, 145.
(14) Husk, D. E.; Seehra, M. S. *Solid State Commun.* **1978**, *27*, 1147.
(15) Schlegel, A.; Wachter, P. *J. Phys. C: Solid State Phys.* **1976**, *9*, 3363.
(16) Peters, E.; Majima, H. *Can. Metall. Q.* **1968**, *7*, 111.
(17) Biegler, T.; Rand, D. A. J.; Woods, R. *J. Electroanal. Chem. Interfacial Electrochem.* **1975**, *60*, 151.
(18) Biegler, T. *J. Electroanal. Chem. Interfacial Electrochem.* **1976**, *70*, 265.
(19) Biegler, T.; Swift, D. A. *Electrochim. Acta* **1979**, *24*, 415.
(20) Meyer, R. E. *J. Electroanal. Chem. Interfacial Electrochem.* **1979**, *101*, 59.
(21) Li, E. K.; Johnson, K. H.; Eastman, D. E.; Freeouf, J. L. *Phys. Rev. Lett.* **1974**, *32*, 470.

0022-3654/91/2095-3682$02.50/0

band energies of the FeS_2 particles.

Experimental Section

Chemicals. FeS_2 (AESAR, 99.9%, Seabrook, NH) powder was ground to a grain size of approximately 10 μm in an agate mortar and used in all experiments. FeS_2/Pt (5% w/w) was prepared by adding 2 g of FeS_2 to 0.1 M sodium potassium tartrate (30 mL) and adjusting the resulting suspension to pH 4. A 6.1-mL sample of a 0.08 M solution of H_2PtCl_6 was added. The suspension was stirred and degassed with N_2 for 1 h and then irradiated for 10 h. The powder was filtered out, washed with water, and air-dried. Na_2S (Aldrich, 98%) solution was freshly prepared before each experiment. Methyl viologen (Sigma) was added directly into the electrochemical cell before the experiment. All other chemicals were reagent grade and were used as received without further purification. All solutions were prepared with water obtained from a Millipore water system.

Apparatus. The electrolysis cell was a 100-mL Pyrex H-cell, divided by a fine-porosity glass frit and equipped with a flat optical window to allow illumination of the entire width of the cell. One compartment housed the working (collector) electrode, a 2-cm^2 platinum-gauze cylinder, and a saturated calomel reference electrode (SCE). The second compartment contained a 5.4-cm^2 platinum counter electrode. This cell was used in all experiments. A Corning Model 701A pH meter was used to measure the pH of the suspension.

Irradiations were performed with the beam from a tungsten–halogen lamp (Sylvania, 650 W) yielding a photon energy density of 0.44 W/cm^2, as determined with an EG&G Model 550-1 radiometer/photometer. The area of irradiation was about 5 cm^2. A water bath with a 13-cm path length was used to filter IR irradiation. All current–time curves were obtained with a Princeton Applied Research (PAR) Model 173 potentiostat, a PAR Model 175 universal programmer, and a Houston Instruments Model 2000 x-y recorder.

Procedure. The experimental procedures basically followed previous practice.[31-34] Typical solutions were prepared by adding 50 mL of the desired solution to a given amount of FeS_2 in the working electrode compartment. All solutions were degassed with prepurified N_2 for 1 h before irradiation. During the degassing process, the solution in the working electrode compartment drained through the frit into the counter electrode compartment until both were at the same liquid level. Since the grain size of FeS_2 was too large to pass through the fine-porosity glass frit, almost all of the FeS_2 suspension remained in the working electrode compartment. Suspensions were stirred with a magnetic stirrer during the measurements. The potential of the working electrode was adjusted to the desired value and irradiation started when the background current reached a constant value. For studies of pH effects, the pH of the test solution was adjusted by addition of small amounts of either 1.0 M HNO_3 or 1.0 M NaOH.

Results

Photocurrent with and without Electron Acceptors. When a stirred FeS_2 suspension (0.375 mg/mL) in a tartrate medium (1 M sodium tartrate, pH 6.6) containing a platinum collector electrode (held at 0 V vs SCE) was illuminated, a small anodic photocurrent (~2 μA) was observed initially. This current increased very slowly, attaining a maximum value of 32 μA in 90 min. The magnitude of the current was independent of the position and orientation of the collector electrode in the cell. However, the photocurrent vs time curves showed some difference between the case when the light beam impinged directly on the collector electrode and that when the beam only irradiated the solution (Figure 1). When the light did not impinge directly on the electrode, the photocurrent increased very slowly during the first 15 min of illumination and after that at a much faster rate. A similar result was found for the case when only solution in the immediate vicinity of the electrode was irradiated, except that the photocurrent observed in the first 15 min of illumination was higher. For both cases, a maximum photocurrent of about 32 μA was observed. These results follow the previously described scheme,[31] where some photogenerated holes are transferred to tartrate ions, leaving electrons on the FeS_2 particles, which can be collected at the inert electrode. The difference in behavior observed with variable positioning of electrodes suggests that a small fraction of the photocurrent results from some FeS_2 particles sticking to the collector electrode surface. The slow buildup of photocurrent suggests that FeS_2 particles with excess electronic charge accumulate in the bulk solution, so that the concentration of oxidizable particles gradually increases. The rate of attainment of the steady-state current depends upon the cell volume and the mass-transfer coefficient.[33]

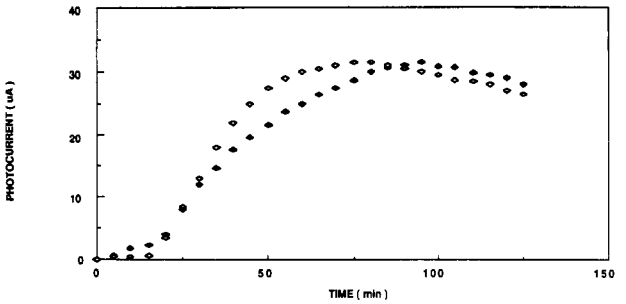

Figure 1. Photocurrent vs time for an FeS_2 suspension: 1.0 M tartrate; 18.75 mg of FeS_2; Pt collector electrode (2 cm^2) at 0 V vs SCE; incident light on the electrode (◇) direct, (◆) indirect.

Since the solution components are stable, the slow decay in photocurrent that starts at about 100 min probably represents decomposition of the FeS_2. This probably represents either a reaction of photogenerated holes with the FeS_2 lattice to produce SO_4^{2-} as a corrosion product[4] occurring in parallel with hole transfer to tartrate ions or a slow reaction of photogenerated electrons. Even after days of illumination, the photocurrent remained finite. From the total amount of FeS_2 and the integrated photocurrent during this period, turnover numbers[33] greater than unity were found.

As reported previously,[32-34] addition of a substance to the solution that is capable of reacting with the photogenerated electrons on the particles to form a reduced product oxidizable at the collector electrode can increase the photocurrent significantly. However, the addition of small amounts (1.0 mM) of methyl viologen (MV^{2+}) to stirred FeS_2 suspensions in 1 M tartrate solution (pH 6.6) or in 1 M acetate solution (pH 7.2) did not result in a large enhancement of the anodic photocurrent when the collector electrode was held at −0.4 V vs SCE. This potential was >200 mV more positive than the cathodic peak potential for reduction of MV^{2+}, as determined by cyclic voltammetry at a Pt electrode before the photoelectrochemical experiment. Under illumination ($h\nu \geq 390$ nm), no appearance of the blue methyl viologen radical cation ($M^{\bullet+}$) was observed. Apparently, at this pH, MV^{2+} cannot be reduced by electrons in the illuminated FeS_2 particles. However, a large enhancement of the photocurrent was observed in the presence of MV^{2+} when the pH of the solution was increased to 12.0, where the quasi-Fermi level of electrons in the FeS_2 particles is at a higher energy (i.e., at a more negative potential). Moreover, when 1 mM $Ru(NH_3)_6^{3+}$, which is a

(22) Khan, M. S. *J. Phys. C: Solid State Phys.* **1976**, *9*, 81.
(23) Sugiura, C. H. *J. Chem. Phys.* **1984**, *80*, 1047.
(24) Liu, C.-Y.; Bard, A. J. *J. Phys. Chem.* **1989**, *93*, 7047.
(25) (a) Bard, A. J. *J. Photochem.* **1979**, *10*, 59. (b) Bard, A. J. *J. Phys. Chem.* **1982**, *86*, 172.
(26) Bard, A. J. *Science (Washington, D.C.)* **1980**, *207*, 139.
(27) Aspnes, D. E.; Heller, A. *J. Phys. Chem.* **1983**, *87*, 4919.
(28) Hodes, G.; Grätzel, M. *Nouv. J. Chim.* **1984**, *8*, 509.
(29) Hodes, G. In *Energy Resources through Photochemistry and Catalysis*; Grätzel, M., Ed.; Academic Press: New York, 1983.
(30) Gerischer, H. *J. Phys. Chem.* **1984**, *88*, 6096.
(31) Ward, M. D.; Bard, A. J. *J. Phys. Chem.* **1982**, *86*, 3599.
(32) Ward, M. D.; White, J. R.; Bard, A. J. *J. Am. Chem. Soc.* **1983**, *105*, 27.
(33) White, J. R.; Bard, A. J. *J. Phys. Chem.* **1985**, *89*, 1947.
(34) Leland, J.; Bard, A. J. *J. Phys. Chem.* **1987**, *91*, 5076, 5083.

TABLE I: Steady-State Photocurrents at Irradiated FeS_2 Suspensions in the Presence of Different Hole and Electron Acceptors[a]

hole acceptor	pH	amt of FeS_2, mg/mL	i_{ss}, μA	electron acceptor
sodium acetate (1 M)	7.2	3.75	13	MV^{2+} (1 mM)
	7.2	3.75	5	none
sodium tartrate (1 M)	6.6	3.75	11	none
	6.6	3.75	32	MV^{2+} (1 mM)
	12.0	3.75	140	MV^{2+} (1 mM)
	12.8	3.75	280	MV^{2+} (1 mM)
	6.6	0.375	450	$Ru(NH_3)_6^{3+}$ (1 mM)
sodium sulfide (1 M)	13.3	0.375	730	none

[a] The collector electrode (Pt) with an area of 2 cm^2 was maintained at a potential where oxidation of the reduced form of the mediator occurred at a mass-transfer-controlled rate (~0.4 V vs SCE for $MV^{2+/+}$, 0 V for $Ru(NH_3)_6^{3+/2+}$, and −0.67 V for S^{2-}).

SCHEME II

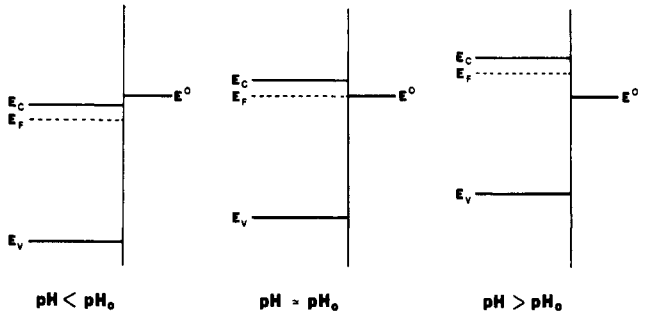

thermodynamically better electron acceptor, was used in the FeS_2/tartrate (1 M) system, a large enhancement of photocurrent was also observed, even at pH 6.6. When $Ru(NH_3)_6^{3+}$ was present as a mediator, there was no decay in the steady-state current with time, such as that shown in Figure 1, which suggests that slow reduction of the FeS_2 by photogenerated electrons is an important component of the current decay process. Values of the steady-state photocurrent (i_{ss}) obtained for several different electron–hole acceptor species are given in Table I. Note that with all of these solutions no photocurrent was observed under illumination in the absence of FeS_2 particles in the cell.

Effect of pH on Photocurrent. As seen in earlier studies,[31-34] the pH affects the observed photocurrent in both the presence and absence of electron acceptors. This can be understood in terms of the shift of the semiconductor conduction band (CB) and valence band (VB) energies as a function of pH. This shift in the electron and hole energies with pH is analogous to the potential shifts observed with solution redox half-reactions that involve exchange of protons. As the pH increases, electrons in the FeS_2 become better reductants and holes become poorer oxidants. This can be represented, for most semiconductors, by Scheme II. As the pH increases, the positions of the bands shift upward with respect to those under vacuum (i.e., the potential of photogenerated electrons becomes more negative). Since the potentials of the redox couples chosen as electron acceptors, $MV^{2+/+}$ and $Ru(NH_3)_6^{3+/2+}$, do not shift with pH, the relative locations of the semiconductor Fermi level and the solution energy level, and hence i_{ss}, depend upon pH, as shown in Scheme II. For example, with MV^{2+} as the mediator at low pH, the conduction band edge was more positive than the standard potential and the i_{ss} observed corresponded to the photocurrent in the absence of an acceptor. When the pH increased, i_{ss} increased. The rate of change of the photocurrent was also a function of pH and increased from 0.44 μA/min at pH 8.7 to 5 μA/min at pH 12.6. The variation of i_{ss} with pH for both redox mediators is shown in Figure 2. The threshold pH for the MV^{2+} system was difficult to determine precisely. However, with $Ru(NH_3)_6^{3+}$, which has a much more positive formal potential (−0.2 V vs SCE) than that of MV^{2+} (−0.69 V vs SCE), a threshold pH of 2.45 was obtained for the FeS_2 particle suspension. This pH value, termed pH_0, is the pH

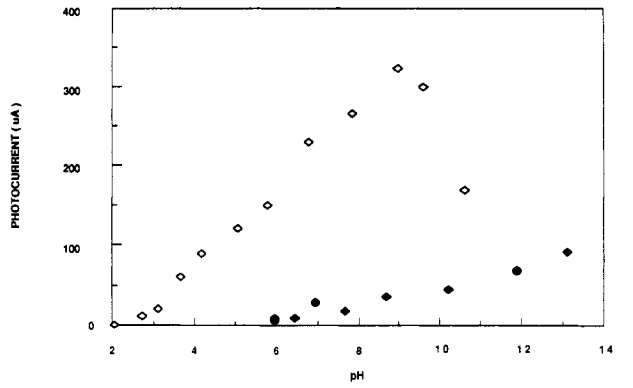

Figure 2. Effect of pH on steady-state photocurrent of FeS_2 suspensions: 18.75 mg of FeS_2; pH adjusted by addition of NaOH or HNO_3; E = 0 V vs SCE; (◆) 1 mM MV^{2+}, 1 M tartrate; (◇) 1 mM $Ru(NH_3)_6$, 0.1 M tartrate. The deviations of each point were about 5 to 10 μA.

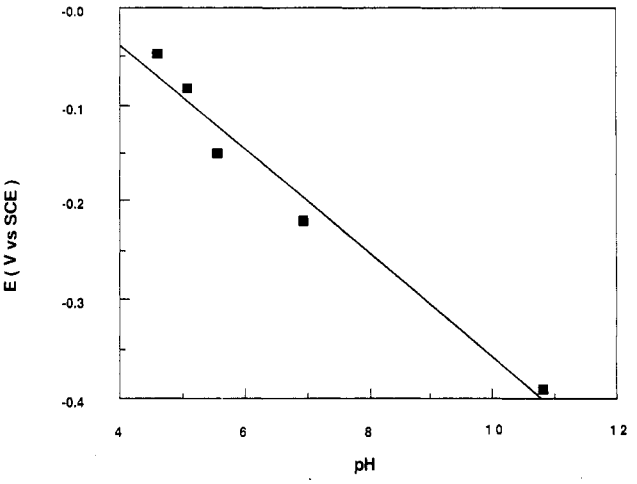

Figure 3. Potential for onset of anodic photocurrent vs pH for FeS_2 suspensions: 1 M tartrate; pH adjusted with NaOH and HNO_3; 40 mg of FeS_2; E = 0 V vs SCE.

at which the onset of photocurrent mediated by the electron acceptor is observed. Below this pH, the mediator makes little contribution to the photocurrent. The drop of the photocurrent for the $Ru(NH_3)_6^{3+}$ system for pH >9 was caused by the instability of $Ru(NH_3)_6^{3+}$ in solution, as confirmed by changes in the UV–visible absorption spectra and the cyclic voltammograms at higher pH values. Note that the FeS_2 particles were very stable in these systems over a pH range of 2–11.

The shifts in the band positions of FeS_2 suspensions as a function of pH were also determined in the absence of an acceptor. The small anodic currents observed in this case correspond to charge transferred directly from the particles to the collector electrode. As the potential of the collector electrode became more negative, the magnitude of the photocurrent decreased and a potential for the onset of current could be estimated. This onset potential became more negative as the pH of the solution increased, as shown in Figure 3. The slope of the line is 59 ± 6 mV/pH unit, which is higher than the value reported for CdS suspensions (40 mV/pH), obtained from a similar experiment,[33] but is about the same as that found with many oxide semiconductors, e.g., TiO_2.

Effect of Sodium Sulfide on Photocurrent. The addition of Na_2S (pH 13.3) resulted in a large enhancement of the anodic photocurrent (up to ca. 1 mA). A control experiment in the absence of FeS_2 particles showed only a very small background photocurrent of less than 10 μA after several hours of illumination. The rate of photocurrent increase on illumination, especially during the early stages, depended on the position of the electrode, as shown in Figure 4. The upper curve represents the case for which the light impinged directly on the electrode. The photocurrent was almost 2 times as high as that found when only solution in the vicinity of the collector electrode was irradiated. However, after long illumination (~1.5 h), the photocurrents in both cases

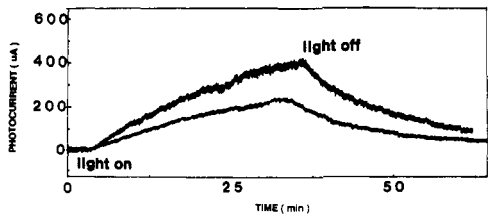

Figure 4. Photocurrent vs time for an FeS_2 suspension: 1.0 M Na_2S; 187.5 mg of FeS_2; Pt collector electrode (2 cm^2) at −0.67 V vs SCE; incident light on the electrode (upper curve) direct, (lower curve) indirect.

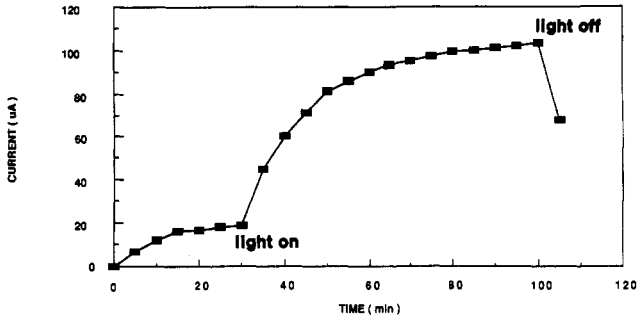

Figure 5. Photocurrent vs time for a Pt collector electrode in 1.0 M Na_2S. The electrode was transferred from the system 1.0 M Na_2S/18.75 mg of FeS_2 after the photocurrent reached steady state under illumination.

reached the same i_{ss} of 730 μA. The color of the solution turned a deeper yellow as the illumination progressed, probably indicating that polysulfide was produced during the process. To understand the surface behavior of the Pt collector electrode, the electrode was removed after the photocurrent reached a steady state. It was then rinsed with water and transferred to a 1 M Na_2S solution. The current in the dark and under illumination is shown in Figure 5. Before illumination, with the electrode held at −0.67 V vs SCE, the background anodic current increased slightly to reach a steady-state value of about 20 μA. With a fresh clean Pt electrode in the same solution, the background current was slightly cathodic. The large increase in i_{ss} found with an electrode that had previously been irradiated in a solution containing FeS_2 suggests that some FeS_2 particles were strongly attached to the Pt surface. To distinguish between physical entrapment of FeS_2 within the Pt-gauze mesh and photoinduced adsorption of FeS_2 particles on the Pt, a clean Pt electrode was dipped into a stirred FeS_2/Na_2S (1 M) solution in the dark for 1 h and then rinsed and transferred to a 1 M Na_2S solution. In this case, as with a clean Pt electrode, the background current in the dark was a small (~3 μA) cathodic one. However, under illumination an anodic photocurrent of 15 μA was produced. This is several times smaller than that found for the same experiment with irradiation of the Pt electrode in the FeS_2 suspension. These results suggest that while some FeS_2 is entrapped in the Pt mesh, a greater quantity becomes attached during the irradiation process (photoadsorption). The observed photocurrent in FeS_2/Na_2S systems consists of components from suspended FeS_2 particles as well as from FeS_2 particles affixed to the Pt surface.

As in studies with other semiconductors, sulfide probably plays the role of the sacrificial donor, reacting with photogenerated holes to produce S_x^{2-}. The cyclic voltammetric behavior of a Pt electrode in a S^{2-}/S_x^{2-} solution is shown in Figure 6. Oxidation of sulfide begins at −0.6 V vs SCE, with reduction of S_x^{2-} occurring at around −0.8 V. The open-circuit voltage (i.e., the rest potential) between SCE and Pt electrodes was measured to be around −0.81 V before illumination. Thus, a Pt electrode immersed in a S^{2-}/S_x^{2-} medium only shows negligible dark current over the potential range of −0.6 to −0.8 V vs SCE. The effect of the addition of 10 mg of FeS_2 in 50 mL of 0.1 M Na_2S on the photocurrent at different electrode potentials is shown in Figure 7. The anodic photocurrent was almost undetectable when the electrode potential was held more negative than −0.70 V vs SCE. When the electrode potential

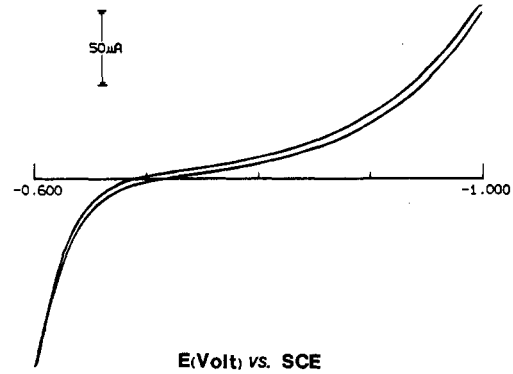

Figure 6. Cyclic voltammogram for the system 1 M Na_2S/1 M S^{2-} with a Pt electrode.

was held more negative than −0.80 V vs SCE, a cathodic current started. Modification of the FeS_2 surface with Pt apparently changed the positions of the energy levels, since the electrode potential for the onset of anodic photocurrent shifted from −0.7 to −0.82 V.

The effect of light intensity for the FeS_2/Na_2S (1 M) system was also studied. The light intensity of the 650-W tungsten–halogen lamp was varied by placing neutral-density filters between the cell and the lamp. Light intensity had a significant effect on the observed photocurrent. A plot of $\Delta i/\Delta t$(initial) vs normalized intensity (I) was fairly linear for the FeS_2/Na_2S (1 M) system (Figure 8).

Discussion

Semiconductor particles of FeS_2 behave as short-circuited photoelectrochemical cells, where both cathodic and anodic reactions occur on the same particle. The electrochemical behavior of FeS_2 suspensions in tartrate solutions generally follows that previously found with TiO_2, CdS, and Fe_2O_3.[31-34] In these experiments, the anodic photocurrent found with illuminated FeS_2 suspensions arises from direct transfer of photogenerated electrons on the particle to the collector electrode, coupled with irreversible removal of holes by tartrate ions. The tartrate ion was an efficient hole scavenger and decomposed upon oxidation to produce CO_2. Evidence of this CO_2 production was the formation of a white precipitate upon addition of an aqueous $Ca(OH)_2$ solution to a 1 M tartrate solution of pH 6.6 following irradiation for 1 h in the presence of FeS_2. Addition of small amounts of the oxidized forms of redox couples (e.g., MV^{2+}, $Ru(NH_3)_6^{3+}$) results in a large enhancement of the photocurrent. This enhancement can be attributed to more efficient scavenging of photogenerated electrons from the particle by solution species and the fast reoxidation rate of these reduced species at the collector electrode.

pH Effects. The effect of pH on i_{ss} for the FeS_2 suspensions in both $MV^{2+/+}$ and $Ru(NH_3)_6^{3+/2+}$ solutions can provide information about the interfacial energetics.[31-34] Since the standard potentials of these two couples are independent of pH in the range studied, any change in photocurrent as a result of a pH change must arise from changes in the energetics of the electrons photogenerated at particle surfaces, as depicted in Scheme II. Adsorption of ions (e.g., H^+, OH^-, HS^-) on particle surfaces results in a shift of the semiconductor band positions in accordance with eq 1, where 0.059 is the slope of the line in Figure 3.

$$E_F = E_F(\text{pH } 0) - 0.059\text{pH} \quad (1)$$

According to the model for variations of i_{ss} of $\Delta i_{ss}/\Delta t$ with pH, the threshold pH, denoted pH_0, is that pH at which the Fermi level (or, more precisely, the quasi-Fermi level for electrons under irradiation, ${}_nE_F^*$) just equals the potential of the redox couple (i.e., −0.20 V vs SCE for $Ru(NH_3)_6^{3+/2+}$). Note that the more negative the potential of the redox couple employed, the higher the pH_0 value expected. The pH_0 for FeS_2 and the $Ru(NH_3)_6^{3+/2+}$ couple was 2.5, which puts ${}_nE_F^*$ at −0.07 V vs SCE at pH 0 and at −0.9 V vs SCE at pH 14.

$${}_nE_F^* = E_{redox} - 0.059(\text{pH} - \text{pH}_0) \quad (2)$$

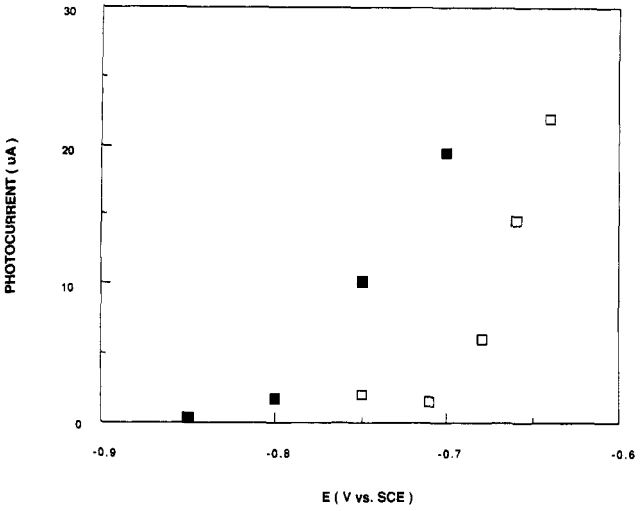

Figure 7. Dependence of photocurrent on electrode potential for stirred FeS_2 (□) and FeS_2/Pt (■) (0.2 mg/mL) suspensions in 0.1 M Na_2S solution. Dark currents were subtracted from the measured photocurrents.

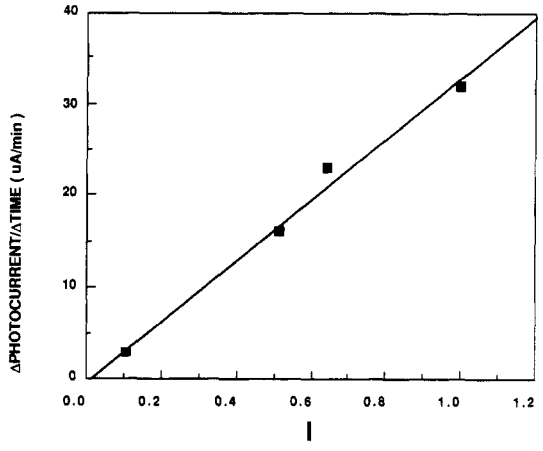

Figure 8. Dependence of rate of change of photocurrent with time in first 15 min of illumination on normalized light intensity for an FeS_2 suspension: 1 M Na_2S; 37.5 mg of FeS_2; Pt electrode at −0.67 V vs SCE.

On the basis of these values and the assumption that the conduction band edge is near ${}_nE_F^*$, the band energies for FeS_2 particles can be estimated, as shown in Figure 9. The estimated pH_0 value for the $MV^{2+/+}$ couple from eq 2 is 11.7. This accounts for the finding that MV^{2+} only becomes a reasonable electron scavenger at pH >12 and suggests that the small photocurrents at pH <12 seen in Figure 2 represent intrinsic FeS_2 electron collection rather than MV^{+} oxidation.

Effect of Sodium Sulfide on Photocurrent. The reason for the large photocurrent produced in Na_2S without the addition of electron acceptor is not clear. However, this system apparently provides excellent stability to the FeS_2 particles, as no decomposition of the semiconductor particles was detected. The steady-state current under illumination remained essentially unchanged for a long period of time (more than 6 h), as shown in Figure 10. Thus, compared to the results in Figure 1, the stability of the FeS_2 is apparently increased by the addition of sulfide. Moreover, the photocurrent was believed to come from the effect of the FeS_2 particles. Although sulfide ion can act as a hole acceptor and imparts excellent stability to the FeS_2 particles under irradiation, the location of the redox potential near the CB edge implies that it is not particularly useful as a sacrificial donor for irradiated FeS_2. Scavenging of electrons by photogenerated S_x^{2-} is also possible, so the fact that reasonable photocurrents are observed in S^{2-} media suggests that the heterogeneous electron-transfer reaction to S_x^{2-} is quite slow. This couple is also quite irreversible at the Pt electrode surface. However, the small potential difference (~0.2 V) between E_C and E_{redox} (S_x^{2-}, S^{2-})

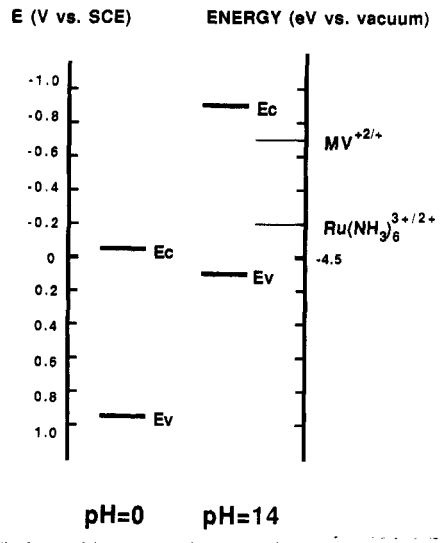

Figure 9. Estimated band energies for FeS_2 suspensions at pH 0 and pH 14.

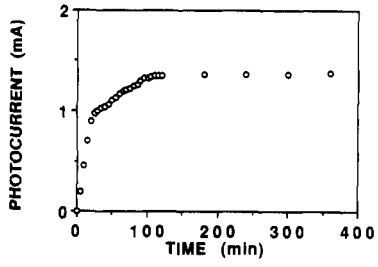

Figure 10. Photocurrent vs time for an FeS_2 suspension: 1.0 M Na_2S; 18.75 mg of FeS_2; Pt collector electrode (2 cm^2) at −0.67 V vs SCE.

suggests that this system is not useful for photochemical energy storage.

The observation of a linear dependence of $\Delta i_{ss}/\Delta t$ on light intensity suggests that e^-/h^+ recombination is not significant under this condition. Deviations from linearity at higher intensities are generally thought to arise from significant e^-/h^+ recombination.[32]

Finally, some of the factors that can affect the performance of the photoelectrochemical cell are discussed. The dimensions of the FeS_2 grains in our experiments (10 μm) are much larger than those of CdS and TiO_2 previously studied. The mobility of these FeS_2 particles is smaller, which thus can lower the rate of transfer to the collector electrode and hence make e^-/h^+ recombination more probable, lowering the photocurrent. Therefore, a higher photocurrent would be predicted with smaller FeS_2 particles. The amount of FeS_2 used was also important in determining the magnitude of the photocurrent. When the amount of FeS_2 was small (e.g., 0.1 mg/mL), the absorbance was small. Hence, most of the light flux passed through the suspension and the efficiency was low. On the other hand, when a large amount of the FeS_2 particles are present, some can be trapped on the Pt-gauze-cylinder electrode and decrease the observed photocurrent. For example, the steady-state photocurrent was 1200 μA for the system FeS_2 (0.375 mg/mL)/Na_2S (1 M), while it was only 500 μA for the system FeS_2 (3.75 mg/mL)/Na_2S (1 M). From our experiments, about 0.5–1 mg/mL is the optimum amount.

Conclusions

We have demonstrated that markedly enhanced photocurrents can be obtained from illuminated FeS_2 suspensions when $Ru(NH_3)_6^{3+}$ is present in the suspension. This behavior is consistent with that revealed in earlier studies of CdS, Fe_2O_3, WO_3, and TiO_2 suspensions; i.e., electron acceptors coupled with efficient hole scavengers are necessary for efficient e^-/h^+ separation and generation of significant photocurrents. The presence of Na_2S in the suspension apparently provides good stability. The variation of

i_{ss} with pH showed that the band energies of FeS_2 suspensions were functions of pH and allowed estimation of the potential of photogenerated electrons (~−0.9 V vs SCE at pH 14). Modification of the surface with Pt can change the position of the energy levels (from −0.81 to −1.01 V for CdS[33]). A similar result was also found for Pt-modified FeS_2 particles.

Acknowledgment. The support of this research by the National Science Foundation (Grant No. CHE8805865) is gratefully acknowledged.

NEXAFS and EELS Study of the Orientation of Sulfur Dioxide on Ag(110)

J. L. Solomon,† R. J. Madix,*

Departments of Chemical Engineering and Chemistry, Stanford University, Stanford, California 94305-5025

W. Wurth, and J. Stöhr

IBM Almaden Research Center, 650 Harry Road, San Jose, California 95120-6099
(Received: August 27, 1990)

The angular dependence of the b_1* resonance in the near-edge X-ray absorption fine-structure (NEXAFS) spectra indicates that the plane of the SO_2 molecule is perpendicular to the plane of the surface and perpendicular to the close-packed direction of the Ag(110) surface ([1$\bar{1}$0] azimuth). SO_2 forms a π-acceptor bond between the $3b_1$ molecular orbital of SO_2 and the Ag(110) surface, and the b_1* resonance corresponds to transitions into the antibonding combination of this π-acceptor bond while still retaining its strong angular dependence on the orientation of the $\vec{E}$ vector. This antbonding combination lies 531.9 eV above the O(1s) level. Off-specular electron energy loss spectroscopy (EELS) measurements confirm the dipole activity of the observed vibrational modes and show that the C_{2v} axis of the SO_2 molecule must be oriented along the surface normal.

Introduction

The adsorption of SO_2 on Ag(110) has been studied previously with temperature-programmed desorption (TPD), low-energy electron diffraction (LEED), ultraviolet and X-ray photoelectron spectroscopy (UPS and XPS),[1] and high-resolution electron energy loss spectroscopy (EELS).[2] These studies showed that SO_2 adsorbs and desorbs molecularly without decomposition or dissociation on the clean Ag(110) surface. At a surface temperature of 100 K multilayers of SO_2 are formed, which desorb in a sharp peak at 120 K. Three desorption states labeled α_1, α_2, and α_3 are also observed at 170, 225, and 275 K, respectively. These states are associated with desorption from the second layer (α_1) and first layer (α_2, α_3), respectively. The binding energies of these states, 41, 53, and 64 kJ mol^{-1}, respectively, indicate significant bonding of the SO_2 molecule to the Ag(110) surface. On the basis of previous EELS measurements, it was suggested that the first layer of SO_2 is bound to the surface via a Ag–S bond, with the plane of the SO_2 molecule tilted toward the surface with the oxygen atoms parallel to the surface, assuming the vibrational modes to be dipole active. This deduction was based on the presence of a mode assigned to the SO_2-Ag out-of-plane wag and the strict application of the surface "selection rule". Indeed the appearance of weak modes, even if they are dipole active, is not necessarily indicative of the orientation of the adsorbed species. The out-of-plane wag of surface-bound SO_2 in fact must exhibit a weak dynamic dipole moment perpendicular to the surface even if metal–molecule charge transfer does *not* accompany the wagging motion. If such charge transfer does occur, as would be expected due to the extensive donation of metal electrons into the π* orbital of SO_2, the wagging motion of an upright SO_2 would become easily observable. The ambiguity of deducing the orientation of the adsorbed SO_2 is thus apparent. Similar conclusions have been reached for the binding of H_2S on Ni(001).[3] To further investigate the orientation of SO_2 on Ag(110), we have measured the near-edge X-ray absorption fine-structure structure (NEXAFS) of SO_2 on Ag(110). The orientation of adsorbed molecules was probed by determining the dependence of transition intensities from the O(1s) level into unoccupied molecular orbitals of the adsorbed species on the angle of incidence of the linearly polarized light.[4] For SO_2 the three lowest unoccupied molecular orbitals in order of increasing energy are the b_1*, a_1*, and b_2*.[5] These transitions are referred to as resonances hereafter.

Xα calculations provide a means of determining the angular dependence of transitions into the unoccupied molecular orbitals.[6] We have carried out such self-consistent calculations for SO_2 using the transition state method, and the results are shown in Figure 1. The potential was constructed by choosing the sphere radii such that the calculated O(1s) ionization potential matched the experimental value. The Xα calculations show that the polarization dependence of the a_1* and b_2* resonances of SO_2 is complicated (compare curves b and c of Figure 1). If the orbital symmetry of the SO_2 molecule were not reduced by the core hole, transitions to a_1* and b_1* would be produced by $\vec{E}$ either in the $\vec{x}$ or $\vec{y}$ directions. From Xα calculations whick take into account the core hole and therefore the symmetry reduction the a_1* resonance is observed only when the $\vec{E}$ is in the $\vec{y}$ direction (Figure 1). The b_2* resonance is observed when $\vec{E}$ is along both the $\vec{x}$ and $\vec{y}$ directions (Figure 1). The angular dependence of the transitions are the result of the local geometry of the molecular orbital on the excited atom, and both the a_1* and the b_2* resonances correspond to transitions into molecular orbitals that have significant intensity in the plane of the molecule (σ symmetry). Due to the complicated angular dependence of these two resonance, they provide little information in determining the orientation of SO_2. However, the Xα calculations also show that the b_1* resonance does not mix with the other resonances, and it remains a valid orbital to determine the $\vec{z}$ direction or, equivalently, the

† Current Address: Process Technologies Laboratory, Building 208-1-01, 3M Center, St. Paul, MN 55144-1000.
* To whom correspondence should be addressed.

(1) Outka, D. A.; Madix, R. J. *Surf. Sci* **1984**, *137*, 242.
(2) Outka, D. A.; Madix, R. J. *Langmuir* **1986**, *2*, 406.
(3) McGrath, R.; MacDowell, A. A.; Hashizume, T.; Sette, F.; Citrin, P. H. *Phys. Rev. B* **1989**, *40*, 9457.
(4) Stöhr, J.; Outka, D. A. *Phys. Rev. B* **1987**, *36*, 7891.
(5) Sze, K. H.; Brion, C. E.; Tong, X. M.; Li, J. M. *Chem. Phys.* **1987**, *115*, 433.
(6) Horsley, J. A. In *Chemistry and Physics of Solid Surfaces*, Vanselow, V. R., Howe, R., Eds.; Springer Series in Surface Science; Springer: Berlin, 1988; Vol. 10.

0022-3654/91/2095-3687$02.50/0